The last five glacial-interglacial transitions: A high-resolution 450,000-year record from the subantarctic Atlantic

G. Cortese,[1] A. Abelmann,[1] and R. Gersonde[1]

Received 23 March 2007; revised 26 June 2007; accepted 12 July 2007; published 19 October 2007.

[1] A submillennial resolution, radiolarian-based record of summer sea surface temperature (SST) documents the last five glacial to interglacial transitions at the subtropical front, southern Atlantic Ocean. Rapid fluctuations occur both during glacial and interglacial intervals, and sudden cooling episodes at glacial terminations are recurrent. Surface hydrography and global ice volume proxies from the same core suggest that summer SST increases prior to terminations lead global ice-volume decreases by 4.7 ± 3.7 ka (in the eccentricity band), 6.9 ± 2.5 ka (obliquity), and 2.7 ± 0.9 ka (precession). A comparison between SST and benthic $\delta^{13}C$ suggests a decoupling in the response of northern subantarctic surface, intermediate, and deep water masses to cold events in the North Atlantic. The matching features between our SST record and the one from core MD97-2120 (southwest Pacific) suggests that the super-regional expression of climatic events is substantially affected by a single climatic agent: the Subtropical Front, amplifier and vehicle for the transfer of climatic change. The direct correlation between warmer ΔT_{site} at Vostok and warmer SST at ODP Site 1089 suggests that warmer oceanic/atmospheric conditions imply a more southward placed frontal system, weaker gradients, and therefore stronger Agulhas input to the Atlantic Ocean.

Citation: Cortese, G., A. Abelmann, and R. Gersonde (2007), The last five glacial-interglacial transitions: A high-resolution 450,000-year record from the subantarctic Atlantic, *Paleoceanography*, *22*, PA4203, doi:10.1029/2007PA001457.

1. Introduction

[2] While periodic changes in the Earth's orbital parameters pace the glacial ages [*Hays et al.*, 1976], many other factors influence the detailed climatic evolution at a specific location at suborbital (centennial to millennial) timescales. The change in oceanic thermohaline circulation (THC) intensity is probably one of the most important of these factors. The evaporative balance of the different oceans plays an important role for the THC: as the Atlantic Ocean loses more moisture (0.32 Sv to the Pacific [*Broecker*, 1997]) than it produces, water must be drawn from other oceans to balance this loss. The two main return water inlets into the Atlantic are the Drake Passage (''cold-water route,'' CWR: South Atlantic Current brings cold water from the Pacific Ocean), and the area south of the Cape of Good Hope (''warm-water route,'' WWR: Agulhas Current brings warm water from the Indian Ocean) (Figure 1). These two water masses mix in the South Atlantic, and the Benguela Current carries this water across the equator, and back to the North Atlantic. A WWR reduction is capable of destabilizing the THC, as it decreases the amount of warm water entering the Atlantic. This affects deep water formation in the North Atlantic, as small changes in temperature, or freshwater input, can tip the balance from conditions in which North Atlantic Deep Water (NADW) forms, to conditions in which it does not [*Pierrehumbert*, 2000].

[3] As THC changes have a direct influence on Pleistocene climate, it is important to understand the role that the Agulhas Current plays in conveying the Indo-Pacific warm water pool toward higher latitudes. Monitoring studies of Agulhas Current flow intensity into the South Atlantic point to an association between increased flux and warmer than usual SSTs [*Agenbag and Shannon*, 1987]. This area is also particularly sensitive to temperature changes, as the southernmost Agulhas Current penetration is associated with the STF position, separating warm, saline subtropical water from cool, low-salinity subpolar water [*Lutjeharms*, 1981]. Currently at about 40°S, the STF location is linked to southern Indian Ocean circulation patterns, and a STF equatorward shift by 4° latitude would altogether prevent Agulhas Current spillage into the Atlantic Ocean, and thus alter the interocean heat budget. There is however debate regarding the intensity of the Agulhas Current during the Last Glacial, as some authors [*Prell et al.*, 1980; *Winter and Martin*, 1990; *Flores et al.*, 1999; *Rau et al.*, 2002; *Gersonde et al.*, 2003a; *Esper et al.*, 2004] support either uninterrupted or seasonally modulated heat transfer from low to high latitudes, while others [*Berger and Vincent*, 1986; *McIntyre et al.*, 1989] suggest it did not retroflect during glacial times. *Peeters et al.* [2004] show how the Agulhas spillage shifts from a strong reduction during mid-glacial times to a vigorous flow during late glacials. Over glacial-interglacial cycles, STF position shifts and wind system rearrangements both directly affect the intensity of the Agulhas spillage, which in turn leaves an imprint on the ODP Site 1089 SST record presented in this paper.

[4] Transfer functions applied to microfossil assemblages have been successfully used to reconstruct past sea surface

[1]Alfred Wegener Institute for Polar and Marine Research (AWI), Bremerhaven, Germany.

0883-8305/07/2007PA001457$12.00

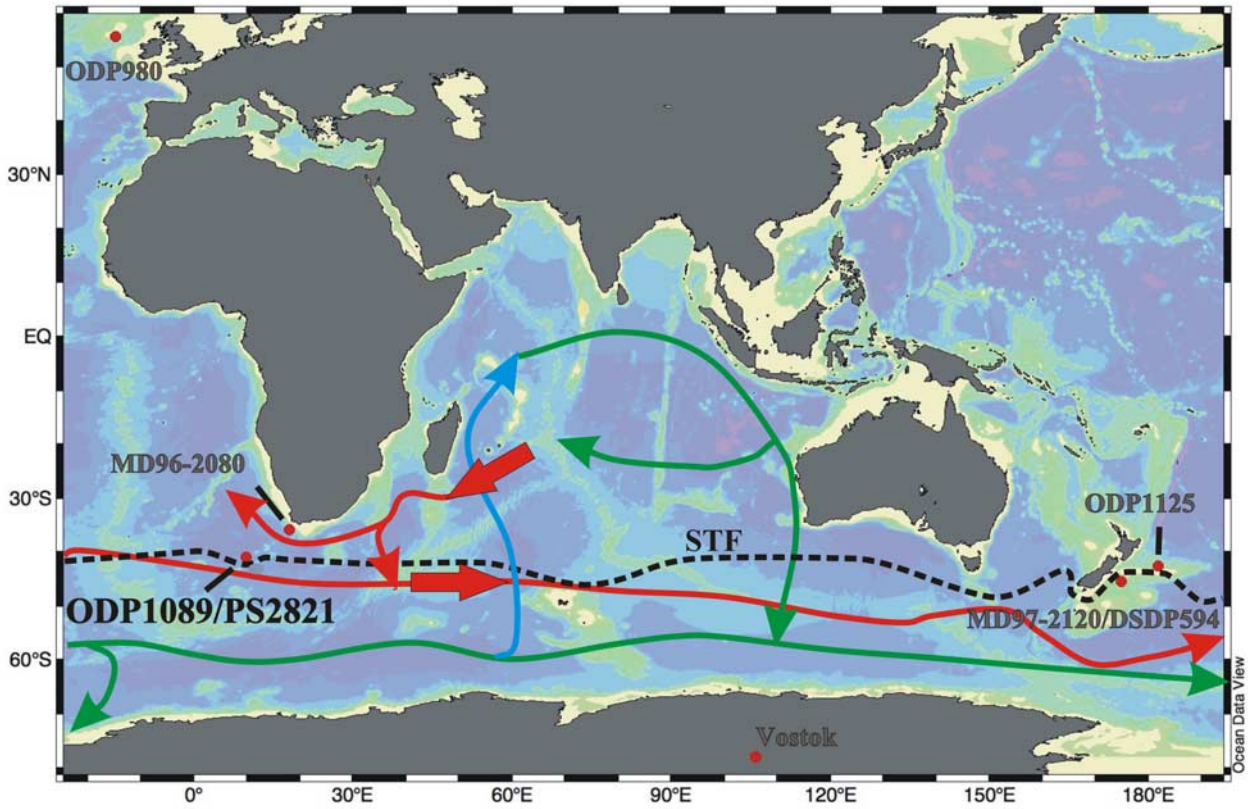

Figure 1. Location of the cores mentioned in the text: ODP Sites 980, 1089, and 1125, PS2821, MD96-2080, MD97-2120, DSDP Site 594, Vostok. The Subtropical Front position (dashed black line, modified after *Belkin and Gordon* [1996]) and the general surface (red), intermediate (green) and deep (cyan) oceanic circulation (adapted from *Schmitz* [1995]) are also shown. The two larger red arrows indicate the inflow of warm surface waters into the Agulhas Retroflection area, and the eastward return flow of surface water south of the Subtropical Front.

temperatures (SST) [*CLIMAP Project Members*, 1981; *Pisias et al.*, 1997; *Zielinski et al.*, 1998; *Abelmann et al.*, 1999; *Cortese and Abelmann*, 2002; *Niebler et al.*, 2003]. Radiolarians are particularly promising in this respect for the study area, as they are highly diversified and well preserved in Southern Ocean sediments [*Brathauer and Abelmann*, 1999; *Cortese and Abelmann*, 2002].

[5] In the latter paper we developed a transfer function to estimate paleoSSTs in the Southern Ocean from radiolarian census data, and applied it to a splice of two cores (ODP Site 1089 and core PS2821-1) recovered from the Subtropical Front (STF) in the South Atlantic. The resulting sub-millennial resolution SST record covered last 160 ka and documented the presence of strong, Dansgaard-Oeschger type climatic instability during MIS 3–4. Rapid cooling episodes (''Younger Dryas-type'' and ''Antarctic Cold Reversal-type'') have been recognized for both Termination I and II.

[6] Planktonic and benthic stable isotopic records (*G. bulloides* and *Cibicidoides* δ^{13}C and δ^{18}O) are available for ODP Site 1089 [*Hodell et al.*, 2003a], and their paleoceanographic interpretation has been discussed in a series of closely related papers. *Ninnemann and Charles* [2002] analyzed benthic foraminiferal oxygen and carbon isotopic records in cores close to Site 1089. They concluded that the substantially lower values of δ^{13}C *Cibicidoides* in the glacial Southern Ocean indicate not only a reduced NADW input to this area during glacial periods, but also a different mode of Southern Ocean deep water formation. *Hodell et al.* [2003b] further suggested, on the basis of benthic δ^{13}C records from Sites 1088, 1089 and 1090, that during glacial times, a chemical divide existed in the Southern Ocean, separating well-ventilated water above 2500 m from poorly ventilated water below. *Mortyn et al.* [2002] discussed, by means of δ^{18}O and δ^{13}C measured on different species of planktonic foraminifera, the surface water structure over two glacial terminations in the Atlantic close to Site 1089. They concluded that the glacial subantarctic was less thermally stratified than it is today.

[7] In this paper, we extend down to ~430 ka the previously published radiolarian-based SST estimates for the spliced Site 1089 and PS2821-1 cores, covering last 160 ka [*Cortese and Abelmann*, 2002]. The time series produced represents a high-resolution climatic record of last five glacial-interglacial cycles located at the boundary between two oceanic regions: the subtropical Indian Ocean and the subantarctic Atlantic Ocean (Figure 1). The analysis of the SST record at this site thus provides clues both about local climatic changes, and those occurring in other regions (Agulhas Retroflection, subantarctic SW Pacific, North Atlantic). The sensitivity of this location to various climate

change mechanisms is due to its proximity to the Subtropical Front, where strong atmosphere/ocean interactions take place, and to the marked influence of the Atlantic/Indian Ocean water exchange through the Agulhas spillage.

[8] We will first discuss the SST record at Site 1089 in terms of its general pattern, the main events recognized, and the structure of Terminations, and then compare it to other climatic proxies from both other oceanic cores and from Antarctic ice cores. The comparison between oceanic, transfer function-derived paleoSST from a Subantarctic site and the deuterium excess record from the Vostok ice core allows us to investigate the controls on the Subantarctic SST history, and recognize possible shifts in the moisture source locations for East Antarctica.

[9] We revise the age models for Sites 1089 and 980, as well as for core MD97-2120, and will then compare our SST reconstruction to similar climatic records from the Agulhas region (core MD96-2080), the southwest Pacific (core MD97-2120, DSDP Site 594 and ODP Site 1125), Antarctica (EPICA Dome C ice core), and the North Atlantic (Site 980) (Figure 1).

2. Material and Methods

[10] Site 1089 (ODP Leg 177) and piston core PS2821-1 (RV *Polarstern* cruise ANT XIV/3) are located beneath the South Atlantic Subtropical Front (40°56′S; 9°54′E, 4620 m water depth and 40°57′S; 9°53′E, 4575 m water depth, respectively, Figure 1). In order to avoid core sections possibly affected by drilling disturbances, the topmost 8.5 meters of piston core PS2821-1 were used instead of the corresponding portion of Site 1089 [*Cortese and Abelmann*, 2002]. We also discuss results from three additional sites for which a detailed reconstruction of the palaeoclimate evolution over several glacial-interglacial cycles is available. Site 980 [*McManus et al.*, 1999] is located in the North Atlantic, core MD96-2080 [*Rau et al.*, 2002] in the southeast Atlantic and core MD97-2120 [*Pahnke and Zahn*, 2005] in the southwest Pacific.

[11] Radiolarian-based SST estimates at Site 1089 were previously presented by *Cortese and Abelmann* [2002] for the topmost 24.49 mcd (meters composite depth), covering last 160 ka. In this paper, we extend that record to 67.57 mcd, corresponding to an age of ~430 ka. A total of 484 levels in the cores, at an average spacing of 14 cm, were sampled. The average time resolution is ~900 years, decreasing to a few hundred years close to Terminations I and II.

[12] Radiolarian slides were prepared according to standard laboratory techniques [*Abelmann et al.*, 1999]. A Zeiss Axioskop microscope, at 160× magnification, was used to determine the relative abundance of radiolarian species, by counting an average of 470 specimens for each slide. The software packages PaleoToolBox and MacTransfer [*Sieger et al.*, 1999] were used to run Q-mode Factor Analysis [*Imbrie and Kipp*, 1971] on radiolarian census data. Details on oceanographic data, statistical properties of the reference data set, and regression equation have been presented elsewhere [*Cortese and Abelmann*, 2002].

[13] Improved age models have been developed only for those sites having a benthic δ^{18}O record. The age model for Site 1089 (Figure 2) was obtained by correlating the *Cibicidoides* δ^{18}O signal from this Site [*Hodell et al.*, 2003a] to the stack of benthic δ^{18}O records of *Lisiecki and Raymo* [2005]. The correlation coefficient between the stack and the Site 1089 *Cibicidoides* δ^{18}O record was 0.94. The age model for the other core we used for comparison (Site 980), has also been developed by correlation to the *Lisiecki and Raymo* [2005] stack. We decided not to tune the age model of core MD97-2120, a Pacific Sector core used for SST comparisons, to our Site 1089 record by peak to peak correlation between the two SST curves (if this were done, the correlation coefficient would be ~0.75). Instead, in order to minimize artificial phase shifts, we used the fixed age points used by *Pahnke et al.* [2003] as a starting point for correlation, and added a few additional tie-points, resulting in a maximum shift between the two records of less than 3 ka over the last 350 ka.

[14] In order to improve the quality of correlation between marine and ice core records, we plotted all data (δD, ΔT_{source}, ΔT_{site}) from the Vostok ice core on the EPICA Dome C (EDC II) age model [*EPICA Community Members*, 2004], which is quite comparable to the *Lisiecki and Raymo* [2005] stack, at least during the past four climate cycles. By doing so, we avoided the occurrence of artificial phase shifts between ice and sediment cores arising from different chronologies. As an example, when comparing the GT4 [*Petit et al.*, 1999] and EDC age models for the Vostok ice core by correlation of the δD record of this core plotted on the two age scales (r = 0.98), the age assignment of a given depth in the Vostok core can shift by as much as 15 kyrs over last 450 ka. Further information on the development of both the marine and ice core age models used in this paper can be found in auxiliary material Figures S1–S3[1].

[15] The Arand software package (P. Howell, Arand software, 1995, freely available from http://pixie.geo.brown.edu/esh/paleo/arand/arand.html) was used to perform Cross Spectral Analysis and to calculate covariance/phases of the time series, while the program AnalySeries [*Paillard et al.*, 1996] was used to correlate between cores. For cross-spectral analysis (80% confidence interval error bar), time series were normalized to unit variance and equally resampled (1 ka sampling interval). The analysis (Figure 3 and Tables 1a and 1b) covered the last 436 ka, and used 131 lags (corresponding to 30% of the series length) and a Bartlett window. A maximum entropy analysis (30% lags) was also applied to the same time series in order to better identify the position of spectral peaks along the frequency scale.

3. Results

3.1. Palaeo-SST Reconstruction

[16] Today's summer SST above Site 1089 (Figure 2) averages 15.7°C, as interpolated from World Ocean Atlas data [*Conkright et al.*, 2002] for the months of December–March. The radiolarian-based SST estimates, having a standard error of estimate of 1.2°C [*Cortese and Abelmann*, 2002], match this value very well, as they predict 15.1°C at 1.8 ka (our youngest sample).

[1]Auxiliary materials are available in the HTML. doi:10.1029/2007PA001457.

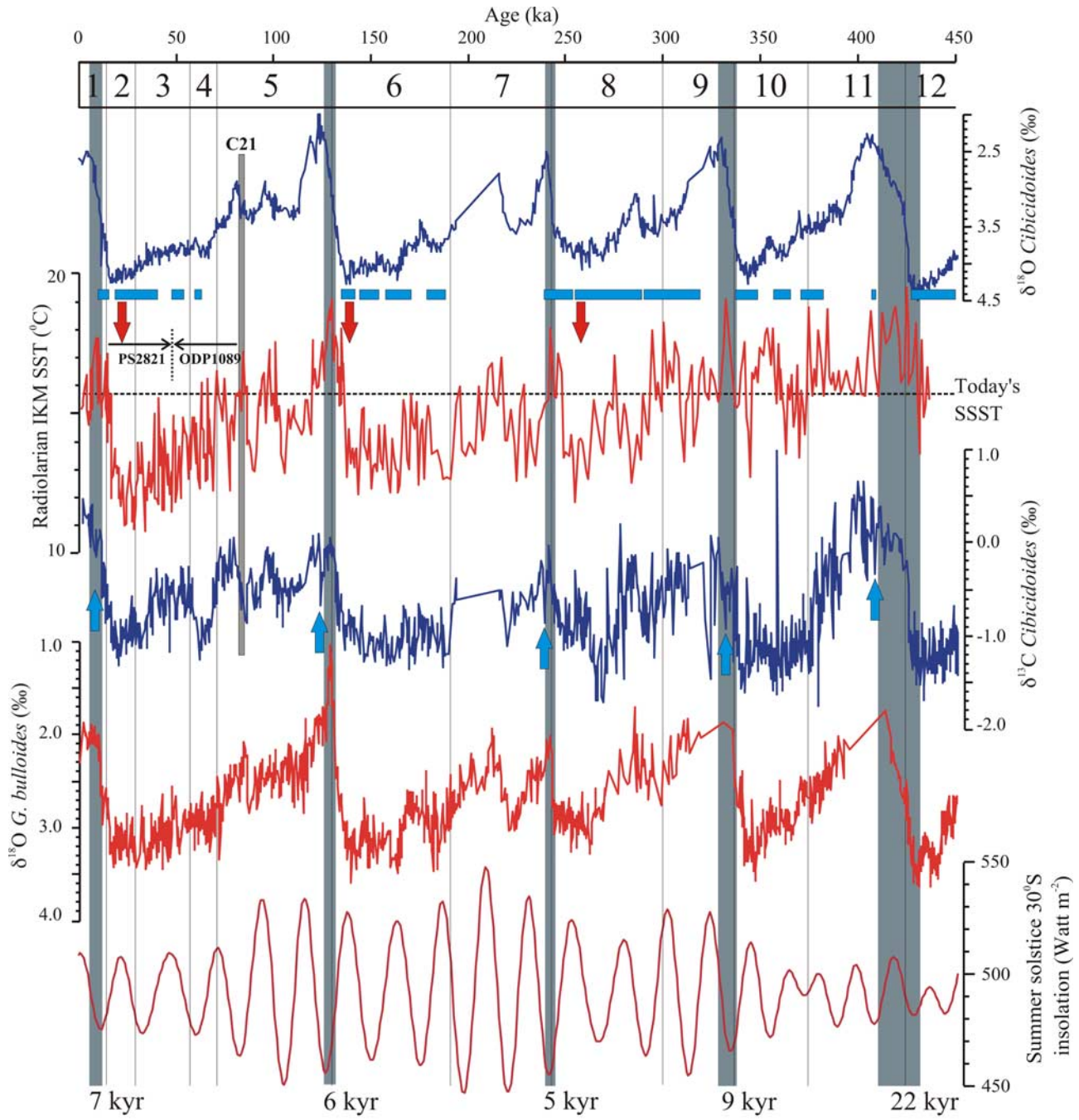

Figure 2. Radiolarian IKM SST, δ^{18}O *G. bulloides,* δ^{18}O and δ^{13}C *Cibicidoides* (in ‰ deviation from the Pee Dee Belemnite standard), summer solstice insolation at 30°S (in Watt m^{-2}). The climatic optima for each glacial cycle are boxed. Today's SST (15.7°C) at Site 1089 location is marked as a dashed line. Marine Isotopic Stages (MIS) are shown on top, boundary ages according to *Lisiecki and Raymo* [2005]. The numbers at the bottom represent the approximate length (in ka) of interglacial optima. Blue arrows indicate δ^{13}C *Cibicidoides* minima right after climatic optimum conditions during interglacials. Important climatic events recognized at core site MD96-2080 [*Rau et al.*, 2002] are also shown: *Globorotalia menardii* accumulation rate peaks at 22, 139, and 258 ka (red arrows), and relative abundances of *Neogloboquadrina pachyderma* (dextral) higher than 20% (blue horizontal bars), see text for discussion. The North Atlantic cooling event C21, at 82–85 ka (terminology after *Chapman and Shackleton* [1999]) is also highlighted.

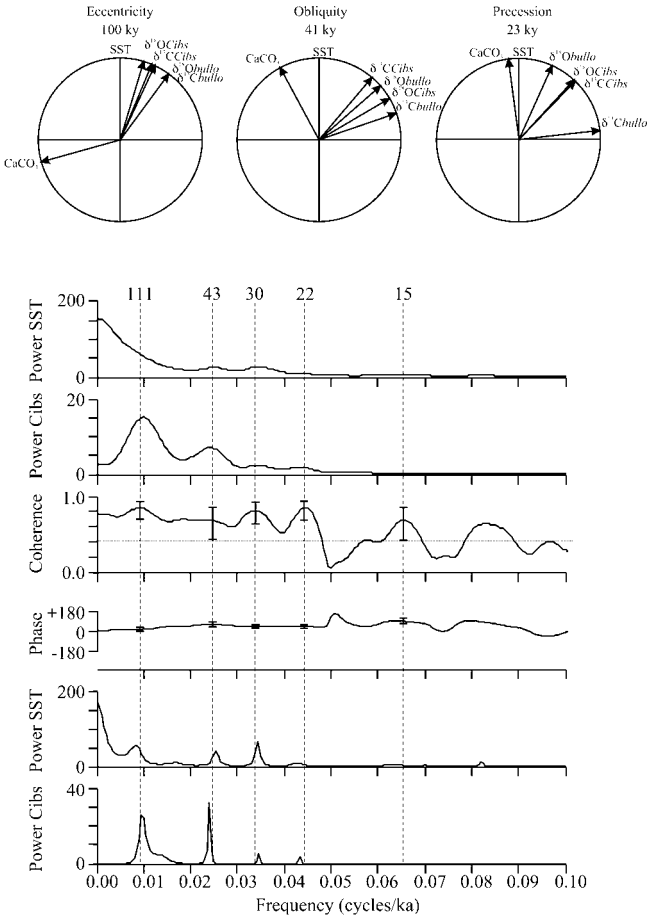

Figure 3. Blackman-Tukey cross spectra (power, coherency, and phase) for Site 1089 SST and δ^{18}O *Cibicidoides*. The input options were as follows: 437 samples, 131 lags (30% of series length), Bartlett Window filtering, 80% confidence interval, series normalized to unit variance and equally resampled at 1 ka interval. The periods of the main peaks (vertical dashed lines) are shown on top. The 80% confidence interval error bars are plotted on the Coherence and Phase diagrams. The two bottom plots are power density spectra for a maximum entropy analysis (30% lags) carried out on the same time series, in order to better identify the position of spectral peaks along the frequency scale, as this technique has better resolution (but lower confidence) compared to the Blackman-Tukey technique. Pie diagrams show the phase relationship, in the eccentricity, obliquity, and precession band, between SST, δ^{18}O and δ^{13}C *G. bulloides,* δ^{18}O and δ^{13}C *Cibicidoides*, and $CaCO_3$%. The data used to construct these diagrams are also shown in Tables 1a and 1b.

[17] The palaeo-SST record displays the last five glacial to interglacial terminations, each having a magnitude of 6°–7°C. We also observe during intervals between 20–70 ka (MIS 2–4) and 140–190 ka (MIS 6) rapid warming episodes (3°–5°C in amplitude) similar to the Dansgaard-Oeschger events (D/O), recognized in Greenland ice cores and in North Atlantic oceanic records [*Martrat et al.*, 2007]. A similar high temperature variability during glacial intervals has also been recently documented for the EPICA Dronning Maud Land ice core [*EPICA Community Members*, 2006], with warm episodes during MIS 3 corresponding to cold events in Greenland.

[18] At Site 1089 (Figure 4), climatic optima generally take place during the initial part of each interglacial interval. However, the past five interglacials display a wide range of duration and amplitude: the climatic optima of MIS 1 and 7 are similar, both 2°C warmer than present and 5 to 7 ka long, while MIS 9 and 11 are 3.5°C warmer and 9 to 22 ka long. The MIS 5 optimum is intermediate both in temperature (3°C warmer) and duration (6 ka).

[19] Another characteristic feature of our paleoclimatic record is the occurrence of cooling rebounds at glacial terminations. These events are present at all last five Terminations, indicating how their occurrence is not limited either spatially (to the North Atlantic), or temporally (to last Termination: MIS 2 to MIS 1).

[20] Our record starts at the transition between MIS 12 and 11, and the first two glacial periods (MIS 10 and 8) display relatively warm and stable conditions, compared to the highly variable MIS 2–4 and 6. The latter two glacial intervals, in fact, have colder average temperatures compared to MIS 8 and 10, but display a marked short-term climatic variability, with sudden, bundled oscillations in temperature. Anomalously high temperatures for a glacial interval characterize MIS 10, as they fall in the range of the highest temperatures reached during two later interglacials (MIS 1 and 7). Termination III (at ~240 ka), although similar to the two previous ones in its duration, the presence of a cooling event, and the attainment of a climatic optimum during its earliest part, introduces a very short-lived optimum, as temperatures quickly drop to values ~3°C colder than today. MIS 2, the last glacial interval, exhibits the coldest temperatures of our record (~11°C). Another noticeable and recurrent feature of the climatic evolution at Site 1089 is the regular occurrence of sharp δ^{13}C *Cibicidoides* decreases directly after the attainment of highest SST at the beginning of interglacial periods (Figure 2).

3.2. Early SST Response at Terminations

[21] Cross-spectral analysis between SST and ocean circulation, global ice volume and surface hydrography proxies (δ^{13}C, δ^{18}O *Cibicidoides* and δ^{18}O/δ^{13}C *G. bulloides*, respectively) from Site 1089, allows us to recognize a lead of the surface hydrography signal compared to the global ice volume signal: the first major increase in SST at Terminations at this Southern Ocean location leads (Figures 3 and 4 and Tables 1a and 1b) global ice volume decrease (as recorded by δ^{18}O *Cibicidoides* peaks measured from the same core) by ~1–9 ka [*Ninnemann and Charles*, 1997; *Hodell et al.*, 2001].

[22] Cross-spectral analysis of the SST and δ^{18}O *Cibicidoides* signals over the last 436 ka at Site 1089 indicates a lead of SST by 4.7 ± 3.7 ka (in the eccentricity frequency band), 6.9 ± 2.5 ka (obliquity), and 2.7 ± 0.9 ka (precession). Similar values for the lead of SST over δ^{18}O *Cibicidoides* (4.9 ± 1.9 ka, 1.6 ± 1.6 ka, 3.0 ± 1.1 ka for the eccentricity, obliquity, and precession band, respectively)

Table 1a. Summary of the Blackman-Tukey Cross-Spectral Analysis Applied to SST and δ^{18}O Cibicidoides: Cross-Spectral Significant Peaks (80% Confidence Level)[a]

Frequency	Period, ka	Power SST	Power Cibs	Coherence	Phase, rad	Phase, deg	Phase, ka
0.0090	111.1	62.96	14.69	0.85	0.27	15.3	4.7
0.0230	43.5	23.22	6.75	0.69	1.03	59.1	7.1
0.0335	29.9	25.92	2.27	0.81	0.80	45.9	3.8
0.0445	22.5	9.44	1.77	0.84	0.73	41.9	2.6
0.0655	15.3	7.36	0.26	0.68	1.60	91.8	3.9

[a]See methods paragraph in section 2 and Figure 3 caption for input options. The first five significant peaks (80% confidence level) are reported, along with their frequency, period, power, and phase (in radians, degrees, and ka). The bottom half of the table shows the coherency (*k*), phase, and error (in degrees (phi) and ka) for SST and δ^{18}O *Cibicidoides* for the three main orbital frequencies.

were obtained by *Becquey and Gersonde* [2003] for core PS2489, from the Subantarctic. The shorter lead recognized by these authors in the obliquity band (~0–3 ka compared to 5–9 ka in our study) might be related to a more "polar," and therefore more affected by obliquity, character of the PS2489 record as this core is located in the southern Subantarctic, compared to the almost subtropical location of Site 1089, where the fastest response is in the precession band.

[23] During terminations, ocean circulation, surface hydrography, and global ice volume proxies from Site 1089 suggest that the SST increase is roughly synchronous to increases in the benthic δ^{13}C signal and both lead the global ice-volume signal by ~1–9 ka.

4. Discussion

4.1. Surface Hydrography Changes Prior to Glacial Terminations

[24] At the past five terminations (Figures 3 and 4), Site 1089 SST leads δ^{18}O *Cibicidoides* (global ice volume proxy) by 4.7 ± 3.7 ka in the eccentricity frequency band, 6.9 ± 2.5 ka (obliquity), and 2.7 ± 0.9 ka (precession). This is an indication of early warming of the surface ocean prior to glacial terminations at this subantarctic South Atlantic location, as SST rose substantially at subantarctic latitudes before any considerable continental ice volume change was recorded. The importance of the lead, and freshwater fluxes into the Southern Ocean, has already been stressed [*Seidov et al.*, 2001], and a similar early response at terminations occurs in the California Current (East Pacific), at subtropical/subboreal latitudes [*Herbert et al.*, 2001], at subantarctic latitudes [*Charles et al.*, 1996; *Labeyrie et al.*, 1996; *Brathauer and Abelmann*, 1999], in the eastern tropical Atlantic Ocean [*Schneider et al.*, 1995], in the SW Africa upwelling system [*Kim et al.*, 2002], and in the Polar and Antarctic Zone as well [*Kunz-Pirrung et al.*, 2002; *Bianchi and Gersonde*, 2002, 2004]. In the California Current region SST increases several kyrs in advance of deglaciation at past glacial maxima [*Herbert et al.*, 2001], suggesting that the surface ocean responded faster than continental ice sheets to an external climatic agent, for example, solar activity changes, sea-ice retreat, atmospheric CO_2 decrease [*Shackleton*, 2000].

[25] The early warming of the surface subantarctic Atlantic waters [*Charles et al.*, 1996], deep Pacific, and surface eastern tropical Pacific, was synchronous with early warming over Antarctica and the Southern Ocean [*Spero and Lea*, 2002]. The connection between North Pacific and subantarctic Southern Ocean is also confirmed by modeling studies indicating a stronger AAIW ventilating the North Pacific during glacial times [*Campin et al.*, 1999] and by the observation that deep Pacific Ocean warming, possibly linked to early warming in Antarctica, preceded major deglaciation, ice sheet melting, and sea level rise [*Mix et al.*, 1999].

[26] The similar early warming response at terminations at subtropical/subantarctic latitudes (California Current and Site 1089) might represent a quick response of intermediate water formation to atmospheric processes. This sensitivity could derive from strong interactions between atmosphere cells and oceanic fronts at these latitudes, acting as powerful climatic feedback mechanisms.

[27] The transfer mechanism of rapid climate change would be mixed, both atmospheric and oceanic: the climate signal (e.g., the temperature rise during a termination) may originate, by direct radiation forcing, in the tropics, an area particularly prone to strong circulation reorganizations [*Pierrehumbert*, 2000], be transported via oceanic circulation or via the atmosphere to the Southern Ocean, and from there, probably through the ventilation of intermediate waters [*Pahnke and Zahn*, 2005], to the rest of the world (e.g., North Atlantic). The surface hydrography lead in our record probably documents one of the early stages of this chain of events, as it integrates the oceanic transport out of

Table 1b. Summary of the Blackman-Tukey Cross-Spectral Analysis Applied to SST and δ^{18}O Cibicidoides: Phase Between SST and δ^{18}O *Cibicidoides* at Orbital Frequencies[a]

	1/100 kyr^{-1}			1/41 kyr^{-1}			1/23 kyr^{-1}		
SST Versus	*k*	phi	ka	*k*	phi	ka	*k*	phi	ka
δ^{18}O *Cibicidoides* inv	0.84	17,1 ± 13,2	4,7 ± 3,7	0.69	60,3 ± 21,7	6,9 ± 2,5	0.82	42,1 ± 14,1	2,7 ± 0,9
δ^{18}O *G. bulloides* inv	0.82	19,6 ± 14,1	5,5 ± 3,9	0.72	48,4 ± 19,9	5,5 ± 2,3	0.72	23,6 ± 19,6	1,5 ± 1,3
δ^{13}C *Cibicidoides*	0.74	19,1 ± 18,7	5,3 ± 5,2	0.73	41,2 ± 18,9	4,7 ± 2,1	0.70	44,1 ± 20,8	2,8 ± 1,3
δ^{13}C *G. bulloides*	0.76	35,7 ± 17,7	9,9 ± 4,9	0.61	70,4 ± 26,7	8,0 ± 3,0	0.78	83,6 ± 16,1	5,3 ± 1,0
$CaCO_3$%	0.73	−105,8 ± 19,2	−29,4 ± 5,3	0.75	−27,7 ± 17,9	−3,2 ± 2,0	0.63	−7,6 ± 25,5	−0,5 ± 1,6

[a]See footnote for Table 1a.

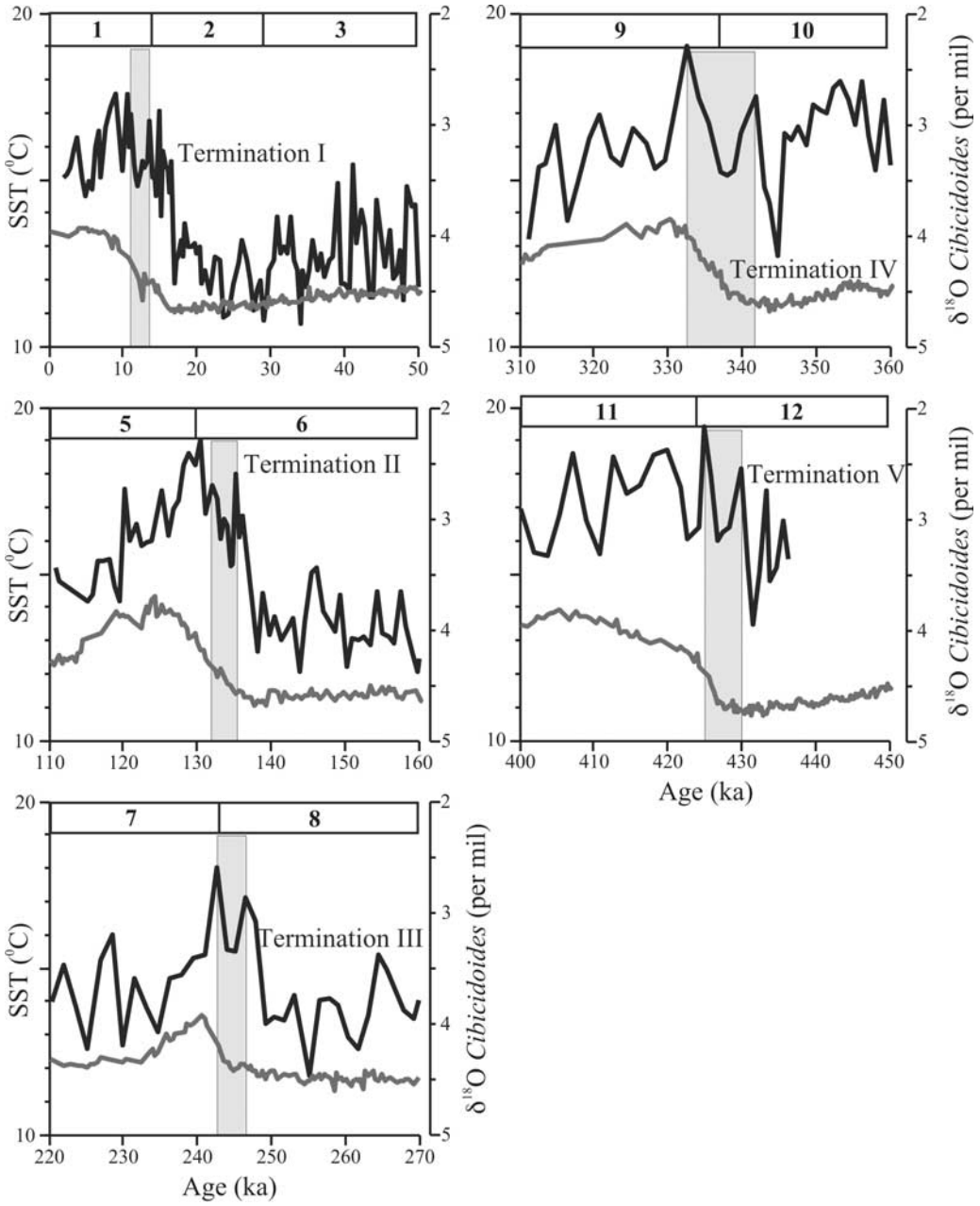

Figure 4. Detail of the SST (in black, this paper) and δ^{18}O *Cibicidoides* (in gray [*Hodell et al.*, 2003a]) evolution at Site 1089 during last five terminations. Cooling events at terminations are highlighted (gray boxes), while Marine Isotopic Stage numbers, according to the *Lisiecki and Raymo* [2005] chronology, are indicated in bold.

the tropics (as the location is affected by the Agulhas Spillage, having its sources at low latitudes in the Indian Ocean) and the ensuing atmospheric transport to high latitudes (regulated by changes in moisture sources to Antarctica, following changes in the position of the STF).

4.2. Cooling Rebounds at Terminations

[28] Our Southern Ocean record shows coolings at each of the last five glacial terminations (Figure 4). Their causes reappear at each deglaciation event, and are not necessarily linked to the occurrence of meltwater discharges in the North Atlantic [*Clark et al.*, 2001]. These cooling rebounds are not present at all terminations in ice core δD-derived temperature records from Antarctica (they appear only at Terminations I and V, Figure 5: ΔT_{site} curve), but they are present at each termination in deuterium excess records from Vostok (Figure 5: ΔT_{source} curve). This is because this signal also incorporates the oceanic signature of lower latitudes, specifically from the source areas for the moisture precipitating in Vostok. They have also been recently documented for some of the last four terminations in a record (MD97-2120) from the subantarctic zone of the southwest Pacific [*Pahnke and Zahn*, 2005], they are also

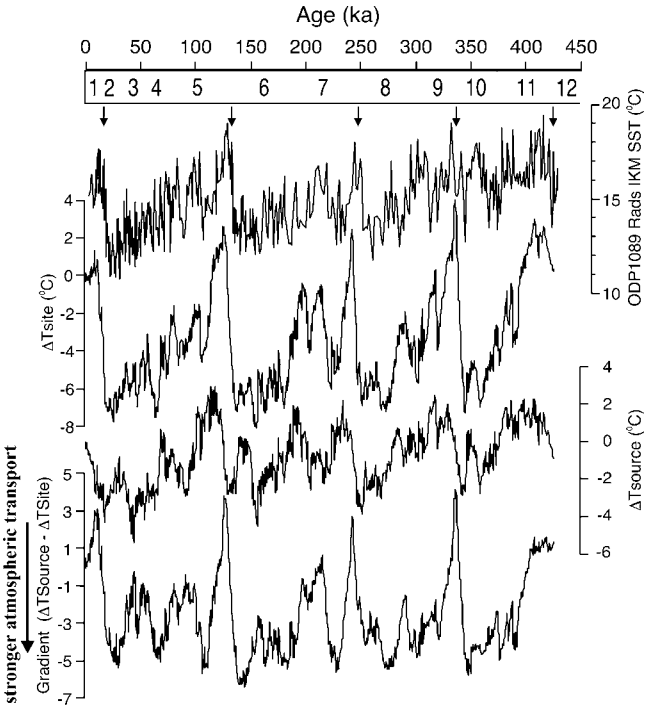

Figure 5. Comparison between SST record of Site 1089 and ΔT_{source}, ΔT_{site} and their gradient from the Vostok ice core, as derived [*Vimeux et al.*, 2002] from deuterium and oxygen isotopes. Vostok data are plotted on the EPICA Dome C (EDC) timescale [*EPICA Community Members*, 2004]. Arrows mark the approximate position of cooling rebounds at glacial terminations.

visible at Sites 1093 and 1094 located south of the APF in the Atlantic Sector [*Kunz-Pirrung et al.*, 2002; *Bianchi and Gersonde*, 2002, 2004], and could therefore be a Southern Ocean feature. The position of the STF (both our and the MD97-2120 records are located just south of it), together with the prevailing wind field and current systems (like the Agulhas Spillage in the South Atlantic) and local meltwater pulses [*Weaver et al.*, 2003], could play a major role in the expression of these cool events during terminations.

[29] Such perturbations of the wind system, and in particular the location of the westerlies belt, took place during the last glacial (and presumably during earlier glacial times as well), and were associated with a northward movement of up to 5° latitude of the oceanographic fronts around Antarctica [*Gersonde et al.*, 2003a, 2003b, 2005].

[30] Additional perturbations of the oceanic circulation occur a few kyr after terminations at Site 1089. These manifest as sharp decreases in the δ^{13}C of *Cibicidoides* following the attainment of optimum temperatures at the beginning of interglacial periods. These anomalies (arrows, Figure 2) were also recognized in the southwest Pacific (core MD97-2120: [*Pahnke and Zahn*, 2005]), and interpreted as regionally (Southern Ocean-) forced ventilation minima.

4.3. Diverging Climatic Trends at 250 ka

[31] The duration of the climatic optimum at interglacials shortens through time (Figure 6). At the same time, the SST record has a slight trend toward decreasing average glacial SSTs, with pre-Termination III (at ~250 kyr) glacial baseline values in MIS 8 and 10 being higher compared to later glacial intervals. Interestingly, the amplitude of the δ^{13}C *Cibicidoides* signal also decreases sharply after Termination III, and glacial baseline values are higher during later glacials (Figure 2), an indication of stronger deep-water ventilation in the Cape Basin during the older half of our record, both during glacials (by CDW) and interglacials (by NADW).

[32] Nannofossils also suggest very different oceanographic conditions at Site 1089 in the time interval older than 250 ka [*Flores et al.*, 2003]. The assemblage suddenly becomes dominated by *Gephyrocapsa caribbeanica*, which frequently reaches ~75% of the nannofossil flora from its Last Common Occurrence (249 ka) to its First Common Occurrence (540 ka). As this species is strongly calcified and represents a warm-water and oligotrophic indicator

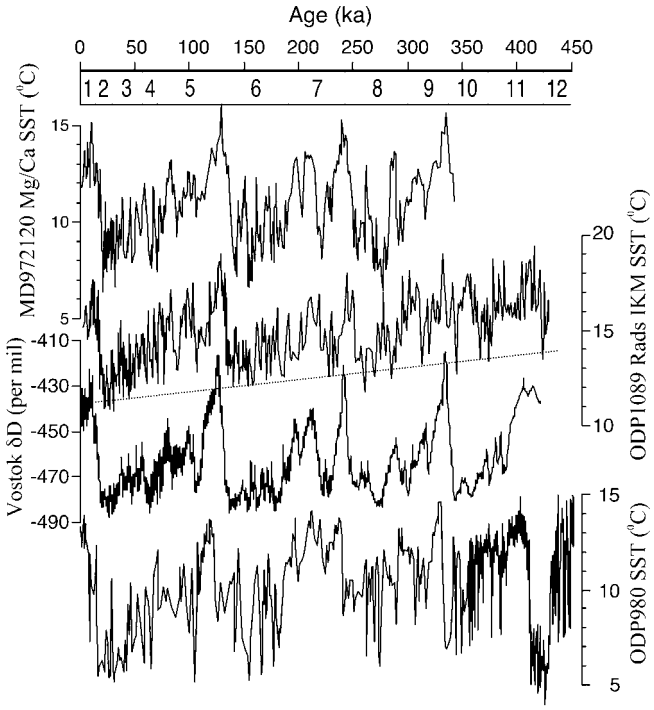

Figure 6. Comparison between the SST records of Sites 980 and 1089, MD97-2120 (see Figure 1 for core positions), and the δD record for the Vostok ice core. Data sources are as follows: Site 980 [*McManus et al.*, 1999], MD97-2120 [*Pahnke and Zahn*, 2005], Vostok ice core [*Petit et al.*, 1999]. Age models for Sites 980 and 1089 have been developed by correlation of their benthic δ^{18}O signal to the *Lisiecki and Raymo* [2005] stack, while the Vostok δD record is plotted on the EPICA Dome C (EDC) timescale [*EPICA Community Members*, 2004]. Core MD97-2120 has been synchronized to Site 1089 by correlation of the two SST records, starting from the tie-points published by *Pahnke et al.* [2003]. See auxiliary material Figures S1–S3 for further information on age models development. The long-term glacial baseline trend in SSTs (dashed line) is indicated for Site 1089.

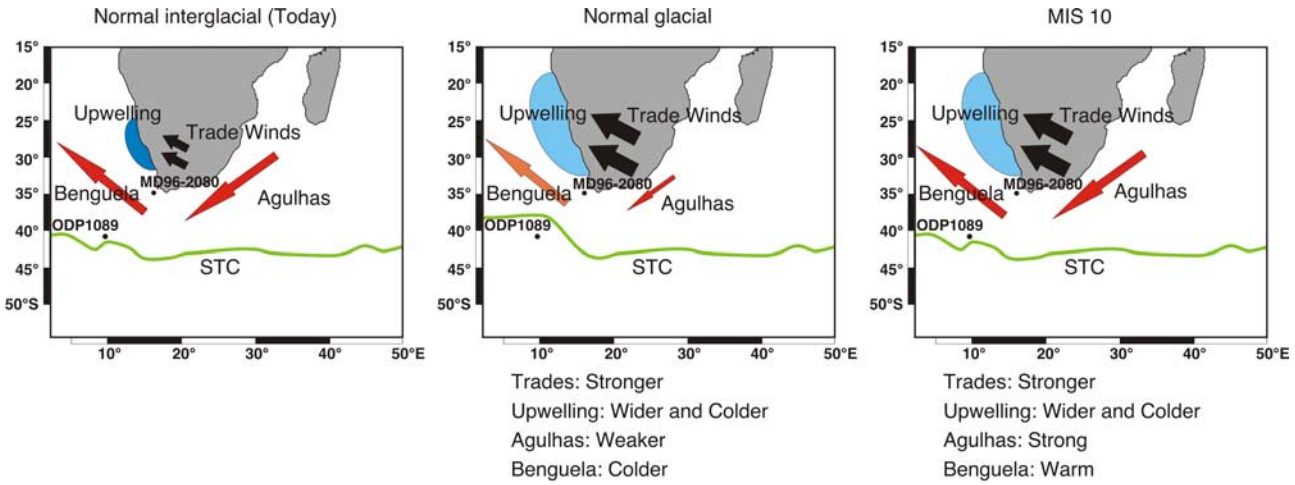

Figure 7. Cartoon of the main climatic mechanisms in the study area during normal interglacial and glacial conditions, and during MIS 10 (warm water anomaly at Site 1089).

[*Flores et al.*, 2003], their findings support our hypothesis for a stronger influence of the Agulhas Current into the Cape Basin earlier than 250 ka. A strong change in surface water conditions in the southeast Atlantic (warmer waters and more clearly defined glacial-interglacial cycles), based on shifts in planktonic foraminiferal assemblages and sediment composition, has also been found at approximately 200–250 ka in core MD96-2080 [*Rau et al.*, 2002], and linked by these authors to a decreased intensity of Agulhas ring shedding and associated subantarctic (cold) water intrusions. The more sustained periods of high SSTs during glacial times earlier than 250 ka at Site 1089 would thus indicate a stronger Agulhas influence into the subantarctic during this time compared to later glacials.

[33] We moreover report elsewhere [*Cortese et al.*, 2004] the presence of an episode of warmer than expected SSTs at Site 1089 during the MIS 10 glacial stage. During this interval, glacial boundary conditions (stronger trade winds and upwelling, driven by intensified atmospheric and oceanic gradients) correspond to a stronger than usual Agulhas Current and a more southern position of the STC (Figure 7). This episode is already "forecast" by the particularly high ΔT_{source} values during MIS 10 at Vostok, which indicate that the moisture source region was also experiencing a strong warming (or migrated to lower latitudes), thus feeding the Agulhas Current with warmer than usual waters for a glacial interval. In particular, MIS 10 (anomalously warm for a full glacial) would be an example of a strong, prolonged Agulhas spillage event, overriding the normal glacial-interglacial cycle.

4.4. Teleconnections and Changes in the Agulhas Retroflection

[34] Our SST record displays strong similarities, both on orbital and millennial scale, with a Mg/Ca-derived SST record (core MD97-2120) from the Pacific Sector, just south of the Subtropical Front [*Pahnke et al.*, 2003] (Figure 6). These similarities concern the large amplitude (up to 8°–9°C) of Terminations, the length and relative intensity of the last four interglacial optima, the occurrence of cooling events during the last portion of each termination, and the very strong variability and marked warmings occurring during the "glacial half" of each climatic cycle. The detailed evolution of each climatic cycle (i.e., the relative magnitude and timing of rapid warmings occurring over the general cooling trend of each cycle) also matches very well between these two widely separated records. Another common trait between Site 1089 and core MD97-2120 is the in-phase behavior of SST and δ^{13}C *Cibicidoides* (Figure 2): most positive SST excursions tend to coincide with higher δ^{13}C values. The reason is that at orbital and millennial scale the SST record of core MD97-2120 is strongly influenced by the intensity of Antarctic Intermediate Water ventilation, and higher SST values generally coincide with heavier benthic δ^{13}C [*Pahnke and Zahn*, 2005].

[35] However, the benthic δ^{13}C record of core MD97-2120 is affected by AAIW, while Site 1089 reflects changes in the properties of Circumpolar Deep Water (CDW) [*Hodell et al.*, 2003a]. Interestingly, in both cores SST and benthic δ^{13}C are covarying at an orbital scale, but there are many exceptions to this coupling at a millennial scale, particularly during glacial intervals. This could represent a decoupling between the reaction of intermediate (AAIW) and deep (CDW) water masses at mid-Southern Hemisphere latitudes to a cooling in the North Atlantic. The interpretation of the benthic δ^{13}C record in terms of intermediate/deep water mass ventilation and the exact synchronization of chronologies for different oceanic cores is problematic. However, it can be interesting to analyze what happens in different areas during a prolonged cold episode in the North Atlantic. In order to do so, we synchronized the two SST curves from core MD97-2120 and Site 1089 (two sites with good SST and benthic δ^{13}C records, indicative of intermediate and deep water conditions in the Southern Ocean, respectively) to within 3 ka over the last 350 ka.

[36] We then chose a particularly long-lasting cooling event occurring during last glacial cycle in the North Atlantic (C21, at 82–85 ka, terminology after *Chapman and Shackleton* [1999]), in order to minimize the possibility for real or artificial (due to dating uncertainties) phase shifts

between the different proxies. The C21 event corresponds to a peak in ice-rafted debris (IRD) abundance and a major drop in benthic δ^{13}C in the North Atlantic (core NEAP18K, *Chapman and Shackleton* [1999]), and correlates well with higher SST and higher benthic δ^{13}C in core MD97-2120 [*Pahnke and Zahn*, 2005, Figure 2]: a perfect example of the bipolar seesaw [*Stocker and Johnsen*, 2003], with meltwater presence in the North Atlantic, sluggish NADW, and lower SST in the North Atlantic corresponding to increased AAIW production and higher SST in the southwest Pacific. The same time interval corresponds, at Site 1089 (Figure 2), to a strong SST peak (indicative of a regional, Southern Ocean response in surface waters), but with a marked minimum in benthic δ^{13}C (weaker CDW in the Atlantic, contrasting with a stronger AAIW in the Pacific, and therefore decoupling between intermediate and deep water masses responses to this cooling event in the North Atlantic). Another line of evidence confirming linkage between bottom water (AABW) overturn and glacial-interglacial climate in the Southern Ocean, at least at an orbital scale, comes from the study of the silt/clay ratio and sortable silt content of Site 1089 [*Kuhn and Diekmann*, 2002]: higher values of these two variables, both indicative of stronger deep water activity, are generally associated with interglacial, warm SSTs. No millennial-scale variability was however detected by these authors in their sortable silt record.

[37] The amplitudes of SST changes at terminations at Site 1089 (6°–7°C for last five terminations) are very similar to what was found by *Schäfer et al.* [2005] at the Subtropical Front, in the southwest Pacific: the amplitudes throughout the last 1 Myr were always greater south (5°–14°C) of the STF than north (2°–7°C) of it, with a trend toward increased amplitudes south of the STF from the early to late Pleistocene. Very similar results were obtained for the warm peaks during the last five interglacials: 2°–3.5°C warmer than present at Site 1089, and 2°–4°C warmer than present at DSDP Site 594. *Schäfer et al.* [2005] also suggest that the STF did not migrate north of its present location during glacials, owing to the frontal system being locked to a submarine high: the Chatham Rise. Instead, they argue for an intensification of the temperature gradient across the front. A similar mechanism can also be assumed for the Cape Basin, where the Agulhas Plateau bounds the position of the STF.

[38] The strong glacial to interglacial SST shifts at terminations we document for the last 450 ka at Site 1089 have also been recognized, on the basis of foraminiferal assemblages, at core site MD96-2080, located leeward of Agulhas Bank [*Rau et al.*, 2002]. The establishment of warmer conditions in the SE Atlantic and southward movement of the STF, clearly seen in the rapid SST increase at terminations at the Site 1089 location, is occurring at times of maximum surface water leakage from the Indian Ocean at the last three glacial terminations, as demonstrated by the occurrence of *Globorotalia menardii* accumulation rate peaks at 22, 139, and 258 ka (Figure 2, red arrows) at core site MD96-2080 [*Rau et al.*, 2002]. At the latter location, higher relative abundances of *Neogloboquadrina pachyderma* (dextral), indicative of peaks in the subantarctic assemblage, represent instead cold water incursions (abundances higher than 20% are reported as blue horizontal bars in Figure 2) over the Agulhas Bank during glacials. The most marked event recorded by *Rau et al.* [2002] in this area is a shift at 200–250 kyr: a mixed northern subantarctic/transitional surface water mass with limited variability on glacial-interglacial cycles during the MIS 12-7 interval is replaced by warmer conditions and more pronounced glacial-interglacial fluctuations. While this change (see section 4.3) and the more pronounced cyclicity starting at 250 kyr are also noticeable at Site 1089 (glacial SSTs are much higher earlier than this turning point compared to later, see Figure 2), the climatic evolution of our record is opposite to the one of core MD96-2080, as glacial intervals at Site 1089 become colder (rather than warmer) and less variable later than 250 kyr. This different climatic evolution indicates a change in the functioning of the Agulhas Retroflection, affecting the northern and southern sides of the STF in opposite ways, and stronger ring shedding intensity during glacials earlier than 250 kyr. This would cause colder conditions north of the STF (cold-core Agulhas rings from the south, core MD96-2080), and warmer conditions south of it (warm-core Agulhas rings from the north, Site 1089).

4.5. Climate Mechanisms

[39] In summary, the available records of climatic evolution over the last four to five climatic cycles at several locations in the ocean (north and south of the STF, both in the Atlantic and Pacific Sectors of the Southern Ocean) display strong similarities both at the orbital scale, and in the detailed variability during glacial intervals, deglaciations, and interglacial climatic optima. These similarities can be explained by the strong influence of the STF at all these locations, while the remaining differences are due to a variety of climatic mechanisms having local importance for some of them (see above and also detailed discussions by both *Schäfer et al.* [2005] and *Rau et al.* [2002]): Agulhas warm-core (Site 1089) and cold-core (MD96-2080) eddy shedding, bottom-topography bounding of the STF position (Site 1125, MD96-2080), incursions of CDW (DSDP Site 594) and SAW (Site 1125), waning of the warm East Cape Current (Site 1125).

[40] The SST record [*McManus et al.*, 1999] from Site 980 (North Atlantic, Feni Drift) also displays several features in common with the SST record of Site 1089. This concerns, in particular, the presence of very warm events (higher than half full interglacial SST values) and sustained intervals of warm temperatures during full glacial periods, as well as an interval of extremely high SSTs centered around ~350 ka, comparable to the Site 1089 MIS 10 warm anomaly [*Cortese et al.*, 2004].

[41] The similarities between some of Vostok climatic indicators (ΔT_{source} and ΔT_{site}) and Site 1089 SSTs would suggest a connection between the subantarctic ocean and Antarctic continent, in the form of moisture exchange, as indicated by models [*Delaygue et al.*, 2000]. The similarities to the southwestern Pacific (MD97-2120), and North Atlantic Ocean (Site 980) records imply further oceanic connection mechanisms. This suggests how the climatic

variability of these widely separated areas can be coupled and covarying at millennial timescales (a few to 10 ka periods), and changes in the intensity of some processes (THC, modulation of Agulhas Current intensity and ring shedding, changes in STF position and strength, wind fields reorganizations during glacials and terminations) have the potential to link the climate response at these locations.

[42] The matching features between our SST record from Site 1089 and the one from core MD97-2120 (its counterpart in the southwest Pacific, as it is also located just south of the STF) provide indication that the super-regional expression of the observed climatic events (terminations, coolings at terminations, warmings during glacial cycles, etc.) should be substantially affected by a single climatic agent. The most likely candidate for such a role, as both core locations lie just to the south of its modern average position, is the Subtropical Front, a very marked boundary in the ocean and also of strong significance for atmospheric circulation, which may act as both an amplifier and a vehicle for the transfer of climatic change between different regions (e.g., Atlantic, Indian, Pacific Sectors of the Southern Ocean, and teleconnections to both Antarctic and Greenland ice sheets). This extraregional connection between mid- and high-southern latitudes has been already proposed on the basis of oceanic records [*Pahnke et al.*, 2003], and is also becoming established thanks to deuterium excess studies, both for the northern and southern hemisphere [*Johnsen et al.*, 1995; *Masson-Delmotte et al.*, 2005; *Vimeux et al.*, 1999, 2001a, 2001b].

4.6. Deuterium-Excess Link: Ice and Marine Records Come Together

[43] The EPICA Dronning Maud Land (EDML) ice core $\delta^{18}O$ record [*EPICA Community Members*, 2006] is a proxy for local temperature on the Antarctic ice sheet. Its overall pattern closely resembles that recorded in most Antarctic ice cores covering the same time period (e.g., $r^2 = 0{,}94$ for the correlation between EDML $\delta^{18}O$ and the EPICA Dome C, EDC hereafter, δD records over the last 150,000 years). Owing to this excellent correlation, and as deuterium excess measurements are not yet available for the last 450 ka from EDML, we will in the following center our discussion on the results from the EDC and Vostok ice cores.

[44] *Delaygue et al.* [2000] demonstrated by GCMs that the moisture source for coastal sites is mostly located in the high-latitude belt of the Southern Ocean, while plateau locations (EDC, Vostok, Dome Fuji) would receive moisture from more distant sources, mostly at subtropical latitudes, in the Indian Ocean. Additionally, moisture source areas change over climatic cycles and affect the deuterium excess signal: the source of moisture for precipitation in Antarctica is located at lower, warmer latitudes during glacial intervals, when the expanded sea-ice cover around Antarctica limits the moisture contribution from high, cold southern latitudes, and the opposite is true during interglacials [*Masson-Delmotte et al.*, 2005].

[45] However, it is still possible to compare the Vostok source temperature signal with oceanic SSTs over a short time interval, assuming that during that period sources remained fixed at a given latitude. Traces of shifts in moisture sources and rearrangements of large-scale atmospheric systems are found in our oceanic paleotemperature record. In fact, ΔT_{site} and Site 1089 SST are positively correlated (Figure 5), probably since warmer conditions imply a more southward placed frontal system, weaker gradients, and therefore stronger Agulhas input to the Atlantic (which is recorded at Site 1089). This condition is typical for interglacial periods, while glacials display the opposite pattern.

[46] At orbital timescale, Site 1089 SST closely follows (Figure 5) the ΔT_{site} record of Vostok, as one can easily correlate most of the features between these two records. However, at suborbital/millennial timescale, glacial intervals and the part of the record older than 350 kyr display a different pattern, as SSTs correlate better to the Vostok $\Delta T_{source} - \Delta T_{site}$ gradient during pre-full glacial times, and to ΔT_{source} (particularly concerning the presence of warm anomalies) during full glacials and the interval preceding 350 kyr. These intervals display, during glacial conditions, warm SST maxima with amplitudes ranging from approximately one third to almost full interglacial values. The presence and degree of expression of these warm SST maxima during full glacial conditions at Site 1089 has interesting climatic implications. In fact, this location should also partly document changes in SST occurring in regions, such as the midlatitude Indian Ocean, that represent both a source of moisture for Vostok, as well as a source of surface waters, advected through the Agulhas spillage, for the site itself. However, particularly during full glacial stages 2 and 6, the oceanic SST maxima, although still present, are relatively minor compared to the reconstructed values for ΔT_{source} [*Vimeux et al.*, 2002]. There are several, some of them concomitant, explanations possible for the lack of an even better match between ΔT_{source} and Site 1089 SST.

[47] 1. The ΔT_{source} signal is of a composite nature, representing the integration of several moisture sources, themselves changing over climatic cycles. Part of this signal is represented by a shift in the predominant moisture source area, which is warmer during glacial times, due to the extended winter sea-ice cover around Antarctica, effectively blocking, at least during this season, moisture input to the continent from higher latitudes. The ΔT_{source} values are higher during full glacial conditions, and must be corrected by taking into account the source shift (as done for Greenland by *Masson-Delmotte et al.* [2005]).

[48] 2. The warmer moisture source is an even more relevant contributor to the precipitation on Antarctica during glacial times, owing to more effective atmospheric transport during glacials, deriving from higher meridional temperature gradients, as also seen in the coincident higher values of the Vostok $\Delta T_{source} - \Delta T_{site}$ gradient.

[49] 3. The SSTs at Site 1089 are only indirectly influenced, via the mediation of the Agulhas Spillage, by temperature changes occurring in the midlatitude Indian Ocean. The very high and prolonged SST maxima during glacial stages 8 and 10 may represent an indication of a different functioning of the Agulhas spillage, with a more direct connection between the prevalent moisture sources to Antarctica (i.e., the midlatitude Indian Ocean) and the

location of Site 1089 (as discussed for MIS 10 by *Cortese et al.* [2004]).

[50] These observations would explain why our SST record matches best the Vostok ΔT_{source} curve in the interval older than ~340 kyr, and suggest that the ΔT_{source} "glacial bump" is representative not only of a major shift toward a warmer moisture source location for Antarctica, but also of warmer than usual waters at low latitudes during this time interval. The expression of this warm anomaly into our Cape Basin oceanic record would be indicative of an "open" Agulhas Spillage, itself anomalous for a glacial time (Figure 7). The general trend toward colder average temperatures and increased climatic variability, with more frequent, but subdued, interstadials during glacial intervals going from MIS 10 to MIS 2 could then be interpreted as the effect, in the study area, of a change in the Agulhas Current regime, going from less to more restricted, with more marked activity pulses during recent glacials.

5. Conclusions

[51] 1. The palaeo-SST record for the last 450,000 years at Site 1089 records rapid temperature fluctuations during both glacial and interglacial intervals.

[52] 2. Brief cooling episodes have been recognized for all last five terminations, directly before the climatic optima of the succeeding interglacials.

[53] 3. The interglacial climatic optima range from 2 to 3.5°C warmer than present, with a duration that can span from as short as 5 ka (MIS 7) to as long as 22 ka (MIS 11).

[54] 4. The first major increase in SST at terminations occurs ~1–9 ka earlier than the decrease in global ice-volume (4.7 ± 3.7 ka, 6.9 ± 2.5 ka, and 2.7 ± 0.9 ka in the eccentricity, obliquity and precession bands, respectively), and most likely corresponds to a stronger advection of warmer waters from the subtropical Indian Ocean via the Agulhas Current.

[55] 5. The SST record displays similarities to both atmospheric (Vostok ice core) and oceanic records from the Southern Hemisphere (cores MD97-2120 and MD96-2080) and Northern Hemisphere (Site 980, Feni Drift), indicating how climatic variability of widely separated areas (the Antarctic continent, temperate North Atlantic and subantarctic South Atlantic and South Pacific) can be strongly coupled and covarying at millennial timescales.

[56] 6. Traces of processes (shifts of moisture sources, rearrangements of large-scale atmospheric systems) affecting the deuterium excess signature of antarctic ice cores have been found in our oceanic paleotemperature record. The occurrence of warmer ΔT_{site} at Vostok in correspondence to warmer SST at Site 1089 suggests that warmer oceanic/atmospheric conditions imply a more southward placed frontal system, weaker gradients, and therefore stronger Agulhas input to the Atlantic (which is recorded at Site 1089).

[57] 7. A comparison between radiolarian- (Site 1089, southeast Atlantic) and Mg/Ca-derived (core MD97-2120, southwest Pacific) SSTs, the corresponding benthic $\delta^{13}C$ records, meltwater and NADW overturn proxies from the North Atlantic supports the seesaw hypothesis: strong oceanic coolings in the North Atlantic correspond to warmings in the surface waters of the northern subantarctic Southern Ocean. However, while intermediate water (AAIW) ventilation seems to be anti-correlated with NADW intensity during these events, the opposite seems true for deeper water masses (CDW), suggesting a decoupled response between surface, intermediate, and deep water masses.

[58] **Acknowledgments.** Core repository facilities (Geology Institute, Bremen University for ODP cores and AWI, Bremerhaven for R/V "Polarstern" cores), are gratefully acknowledged. We would like to thank, for their suggestions and comments, the editor (Gerald Dickens) and the final reviewers: Øyvind Hammer and Chris Hollis, as well as Françoise Vimeux for several interesting and helpful comments over a previous version of this manuscript. Samples for this study were provided by the Ocean Drilling Program (ODP), sponsored by the U.S. National Science Foundation (NSF) and participating countries, under the management of the Joint Oceanographic Institutions (JOI). We thank Ute Bock, Ruth Cordelair, and Tanja Pollak for providing laboratory assistance. This research was supported by the DFG-Research Center "Ocean Margins" of the University of Bremen.

References

Abelmann, A., U. Brathauer, R. Gersonde, R. Sieger, and U. Zielinski (1999), Radiolarian-based transfer function for the estimation of sea surface temperatures in the Southern Ocean (Atlantic sector), *Paleoceanography*, *14*, 410–421.

Agenbag, J. J., and L. V. Shannon (1987), A preliminary note on a recent perturbation in the Agulhas Current retroflexion area, *Trop. Ocean Atmos. Newsl.*, *37*, 10–11.

Becquey, S., and R. Gersonde (2003), A 0.55-Ma paleotemperature record from the Subantarctic zone: Implications for Antarctic Circumpolar Current development, *Paleoceanography*, *18*(1), 1014, doi:10.1029/2000PA000576.

Belkin, I. M., and A. L. Gordon (1996), Southern Ocean fronts from the Greenwich meridian to Tasmania, *J. Geophys. Res.*, *101*, 3675–3696.

Berger, W. H., and E. Vincent (1986), Sporadic shutdown of North Atlantic deep-water production during Glacial Holocene transition?, *Nature*, *325*, 53–55.

Bianchi, C., and R. Gersonde (2002), The Southern Ocean surface between Marine Isotope Stages 6 and 5d: Shape and timing of climate changes, *Palaeogeogr. Palaeoclimatol. Palaeoecol.*, *187*, 151–177.

Bianchi, C., and R. Gersonde (2004), Climate evolution at the last deglaciation: The role of the Southern Ocean, *Earth Planet. Sci. Lett.*, *228*, 407–424.

Brathauer, U., and A. Abelmann (1999), Late Quaternary variations in sea surface temperatures and their relationships to orbital forcing recorded in the Southern Ocean (Atlantic sector), *Paleoceanography*, *14*, 135–148.

Broecker, W. S. (1997), Thermohaline circulation, the Achilles heel of our climate system: Will man-made CO_2 upset the current balance?, *Science*, *278*, 1582–1588.

Campin, J. M., T. Fichefet, and J. C. Duplessy (1999), Problems with using radiocarbon to infer ocean ventilation rates for past and present climates, *Earth Planet. Sci. Lett.*, *165*, 17–24.

Chapman, M. R., and N. J. Shackleton (1999), Global ice-volume fluctuations, North Atlantic ice-rafting events, and deep-ocean circulation changes between 130 and 70 ka, *Geology*, *27*, 795–798.

Charles, C. D., J. Lynch-Stieglitz, U. S. Ninnemann, and R. G. Fairbanks (1996), Climate connections between the hemisphere revealed by deep sea sediment core/ice core correlations, *Earth Planet. Sci. Lett.*, *142*, 19–27.

Clark, P. U., S. J. Marshall, G. K. C. Clarke, S. W. Hostetler, J. M. Licciardi, and J. T. Teller (2001), Freshwater forcing of abrupt climate change during the last glaciation, *Science*, *293*, 283–287.

CLIMAP Project Members (1981), Seasonal reconstructions of the Earth's surface at the Last Glacial Maximum, *Map Chart Ser. MC-36*, Geol. Soc. of Am., Boulder, Colo.

Conkright, M. E., R. A. Locarnini, H. E. Garcia, T. D. O'Brien, T. P. Boyer, C. Stephens, and J. I. Antonov (2002), World Ocean Atlas 2001: Objective analyses, data statistics, and figures, CD-ROM documentation, *Internal Rep. 17*, 17 pp., NOAA, Silver Spring, Md.

Cortese, G., and A. Abelmann (2002), Radiolarian-based paleotemperatures during the last 160 kyrs at ODP Site 1089 (Southern Ocean, Atlantic Sector), *Palaeogeogr. Palaeoclimatol. Palaeoecol.*, *182*, 259–286.

Cortese, G., A. Abelmann, and R. Gersonde (2004), A glacial warm water anomaly in the subantarctic Atlantic Ocean, *Earth Planet. Sci. Lett.*, *222*, 767–778.

Delaygue, G., V. Masson, J. Jouzel, R. D. Koster, and R. Healey (2000), The origin of Antarctic precipitation: A modelling approach, *Tellus, Ser. B*, *52*, 19–36.

EPICA Community Members (2004), Eight glacial cycles from an Antarctic ice core, *Nature*, *429*, 623–628.

EPICA Community Members (2006), One-to-one coupling of glacial Greenland and Antarctica, *Nature*, *444*, 195–198, doi:110.1038/nature05301.

Esper, O., G. J. M. Versteegh, K. A. F. Zonneveld, and H. Willems (2004), A palynological reconstruction of the Agulhas Retroflection (South Atlantic Ocean) during the Late Quaternary, *Global Planet. Change*, *41*, 31–62.

Flores, J. A., R. Gersonde, and F. J. Sierro (1999), Pleistocene fluctuations in the Agulhas Current retroflection based on the calcareous plankton record, *Mar. Micropaleontol.*, *37*, 1–22.

Flores, J. A., M. Marino, F. J. Sierro, D. A. Hodell, and C. D. Charles (2003), Calcareous plankton dissolution pattern and coccolithophore assemblages during the last 600 kyr at ODP Site 1089 (Cape Basin, South Atlantic): Paleoceanographic implications, *Palaeogeogr. Palaeoclimatol. Palaeoecol.*, *196*, 409–426.

Gersonde, R., et al. (2003a), Last glacial sea-surface temperatures and sea-ice extent in the Southern Ocean (Atlantic-Indian sector): A multiproxy approach, *Paleoceanography*, *18*(3), 1061, doi:10.1029/2002PA000809.

Gersonde, R., A. Abelmann, G. Cortese, S. Becquey, C. Bianchi, U. Brathauer, H.-S. Niebler, U. Zielinski, and J. Pätzold (2003b), The late Pleistocene South Atlantic and Southern Ocean surface waters—A summary of time slice and time series studies, in *The South Atlantic in the Late Quaternary: Reconstruction of Material Budget and Current Systems*, edited by G. Wefer, S. Mulitza, and V. Ratmeyer, pp. 499–529, Springer, Berlin.

Gersonde, R., X. Crosta, A. Abelmann, and L. Armand (2005), Sea-surface temperature and sea ice distribution of the Southern Ocean at the EPILOG Last Glacial Maximum—A circum-Antarctic view based on siliceous microfossil records, *Quat. Sci. Rev.*, *24*, 869–896.

Hays, J. D., J. Imbrie, and N. J. Shackleton (1976), Variations in the Earth's orbit: Pacemaker of the ice ages, *Science*, *194*, 1121–1132.

Herbert, T. D., J. D. Schuffert, D. Andreasen, L. Heusser, M. Lyle, A. Mix, A. C. Ravelo, L. D. Stott, and J. C. Herguera (2001), Collapse of the California Current during glacial maxima linked to climate change on land, *Science*, *293*, 71–76.

Hodell, D. A., C. D. Charles, and F. J. Sierro (2001), Late Pleistocene evolution of the ocean's carbonate system, *Earth Planet. Sci. Lett.*, *192*, 109–124.

Hodell, D. A., C. D. Charles, J. H. Curtis, P. G. Mortyn, U. S. Ninnemann, and K. A. Venz (2003a), Data report: Oxygen isotope stratigraphy of ODP Leg 177 Sites 1088, 1089, 1090, 1093, and 1094, *Proc. Ocean Drill. Program Sci. Results*, *177*, 1–26. (Available at http://www-odp.tamu.edu/publications/177_SR/chap_09/chap_09.htm)

Hodell, D. A., K. A. Venz, C. D. Charles, and U. S. Ninnemann (2003b), Pleistocene vertical carbon isotope and carbonate gradients in the South Atlantic sector of the Southern Ocean, *Geochem. Geophys. Geosyst.*, *4*(1), 1004, doi:10.1029/2002GC000367.

Imbrie, J., and N. G. Kipp (1971), A new micropaleontological method for quantitative paleoclimatology: Application to a late Pleistocene Caribbean core, in *Late Cenozoic Glacial Ages*, edited by K. Turekian, pp. 71–181, Yale Univ. Press, New Haven, Conn.

Johnsen, S. J., D. Dahl-Jensen, W. Dansgaard, and N. Gundestrup (1995), Greenland palaeotemperatures derived from GRIP bore hole temperature and ice core isotope profiles, *Tellus, Ser. B*, *47*, 624–629.

Kim, J. H., R. R. Schneider, P. J. Müller, and G. Wefer (2002), Interhemispheric comparison of deglacial sea-surface temperature patterns in Atlantic eastern boundary currents, *Earth Planet. Sci. Lett.*, *194*, 383–393.

Kuhn, G., and B. Diekmann (2002), Late Quaternary variability of ocean circulation in the southeastern South Atlantic inferred from the terrigenous sediment record of a drift deposit in the southern Cape Basin (ODP Site 1089), *Palaeogeogr. Palaeoclimatol. Palaeoecol.*, *182*, 287–303.

Kunz-Pirrung, M., R. Gersonde, and D. A. Hodell (2002), Mid-Brunhes century-scale diatom sea surface temperature and sea ice records from the Atlantic sector of the Southern Ocean (ODP Leg 177, Sites 1093, 1094 and core PS2089-2), *Palaeogeogr. Palaeoclimatol. Palaeoecol.*, *182, 305–328.*

Labeyrie, L. D., et al. (1996), Hydrographic changes of the Southern Ocean (southeast Indian sector) over the last 230 kyr, *Paleoceanography*, *11*, 57–76.

Lisiecki, L. E., and M. E. Raymo (2005), A Pliocene-Pleistocene stack of 57 globally distributed benthic $d^{18}O$ records, *Paleoceanography*, *20*, PA1003, doi:10.1029/2004PA001071.

Lutjeharms, J. R. E. (1981), Features of the southern Agulhas current circulation from satellite remote sensing, *S. Afr. J. Sci.*, *77*, 231–236.

Martrat, B., J. O. Grimalt, N. J. Shackleton, L. de Abreu, M. A. Hutterli, and T. F. Stocker (2007), Four climate cycles of recurring deep and surface water destabilizations on the Iberian Margin, *Science*, *317*, 502–507, doi:10.1126/science.1139994.

Masson-Delmotte, V., J. Jouzel, A. Landais, M. Stievenard, S. J. Johnsen, J. W. C. White, M. Werner, A. Sveinbjornsdottir, and K. Fuhrer (2005), GRIP deuterium excess reveals rapid and orbital-scale changes in Greenland moisture origin, *Science*, *309*, 118–121.

McIntyre, A., W. F. Ruddiman, K. Karlin, and A. C. Mix (1989), Surface water response of the equatorial Atlantic to orbital forcing, *Paleoceanography*, *4*, 19–55.

McManus, J. F., D. W. Oppo, and J. L. Cullen (1999), A 0.5-million-year record of millennial-scale climate variability in the North Atlantic, *Science*, *283*, 971–975.

Mix, A. C., D. C. Lund, N. G. Pisias, P. Bodén, L. Bornmalm, M. Lyle, and J. Pike (1999), Rapid climate oscillations in the Northeast Pacific during the last deglaciation reflect Northern and Southern Hemisphere sources, in *Mechanisms of Global Climate Change at Millennial Time Scales*, *Geophys. Monogr. Ser.*, vol. 112, edited by P. U. Clark, R. S. Webb and L. D. Keigwin, pp. 127–148, AGU, Washington, D. C.

Mortyn, P. G., C. D. Charles, and D. A. Hodell (2002), Southern Ocean upper water column structure over the last 140 kyr with emphasis on the glacial terminations, *Global Planet. Change*, *34*, 241–252.

Niebler, H. S., S. Mulitza, B. Donner, H. Arz, J. Pätzold, and G. Wefer (2003), Sea-surface temperatures in the equatorial and South Atlantic Ocean during the Last Glacial Maximum (23–19 ka), *Paleoceanography*, *18*(3), 1069, doi:10.1029/2003PA000902.

Ninnemann, U. S., and C. D. Charles (1997), Regional differences in quaternary Subantarctic nutrient cycling: Link to intermediate and deep water ventilation, *Paleoceanography*, *12*, 560–567.

Ninnemann, U. S., and C. D. Charles (2002), Changes in the mode of Southern Ocean circulation over the last glacial cycle revealed by foraminiferal stable isotopic variability, *Earth Planet. Sci. Lett.*, *201*, 383–396.

Pahnke, K., and R. Zahn (2005), Southern hemisphere water mass conversion linked with North Atlantic climate variability, *Science*, *307*, 1741–1746.

Pahnke, K., R. Zahn, H. Elderfield, and M. Schulz (2003), 340,000-year centennial-scale marine record of Southern Hemisphere climatic oscillation, *Science*, *301*, 948–952.

Paillard, D., L. Labeyrie, and P. Yiou (1996), Macintosh program performs time-series analysis, *Eos Trans. AGU*, *77*, 379.

Peeters, F. J. C., R. Acheson, G. J. A. Brummer, W. P. M. de Ruijter, R. R. Schneider, G. M. Ganssen, E. Ufkes, and D. Kroon (2004), Vigorous exchange between the Indian and Atlantic oceans at the end of the past five glacial periods, *Nature*, *430*, 661–665.

Petit, J. R., et al. (1999), Climate and atmospheric history of the past 420,000 years from the Vostok ice core, Antarctica, *Nature*, *399*, 429–436.

Pierrehumbert, R. T. (2000), Climate change and the tropical Pacific: The sleeping dragon wakes, *Proc. Natl. Acad. Sci.*, *97*, 1355–1358.

Pisias, N. G., A. Roelofs, and M. Weber (1997), Radiolarian-based transfer functions for estimating mean surface ocean temperatures and seasonal range, *Paleoceanography*, *12*, 365–379.

Prell, W. L., W. H. Hutson, D. F. Williams, A. W. H. Bé, K. Geitzenauer, and B. Molfino (1980), Surface circulation of the Indian Ocean during the Last Glacial Maximum, approximately 18,000 yr B. P., *Quat. Res.*, *14*, 309–336.

Rau, A. J., J. Rogers, J. R. E. Lutjeharms, J. Giraudeau, J. A. Lee-Thorp, M.-T. Chen, and C. Waelbroeck (2002), A 450-kyr record of hydrological conditions on the western Agulhas Bank slope, south of Africa, *Mar. Geol.*, *180*, 183–201.

Schäfer, G., J. S. Rodger, B. W. Haywarda, J. P. Kennett, A. T. Sabaa, and G. H. Scott (2005), Planktic foraminiferal and sea surface temperature record during the last 1 Myr across the Subtropical Front, southwest Pacific, *Mar. Micropaleontol.*, *54*, 191–212.

Schmitz, W. J. (1995), On the interbasin-scale thermohaline circulation, *Rev. Geophys.*, *33*, 151–173.

Schneider, R. R., P. J. Müller, G. Ruhland, G. Meinecke, H. Schmidt, and G. Wefer (1995), Late Quaternary surface temperatures and productivity in the east-equatorial South Atlantic: Response to changes in trade/monsoon wind forcing and surface water advection, in *The South Atlantic: Present and Past Circulation*, edited by G. Wefer et al., pp. 527–551, Springer, Berlin.

Seidov, D., E. Barron, and B. J. Haupt (2001), Meltwater and the global ocean conveyor:

Northern versus southern connections, *Global Planet. Change*, *30*, 257–270.

Shackleton, N. (2000), The 100,000-year ice-age cycle identified and found to lag temperature, carbon dioxide, and orbital eccentricity, *Science*, *289*, 1897–1902.

Sieger, R., R. Gersonde, and U. Zielinski (1999), A new extended software package for quantitative paleoenvironmental reconstructions, *Eos Trans. AGU Electron. Suppl.*, 11 May. (Available at http://www.agu.org/eos_elec/98131e.html)

Spero, H. J., and D. W. Lea (2002), The cause of carbon isotope minimum events on glacial terminations, *Science*, *296*, 522–525.

Stocker, T. F., and S. J. Johnsen (2003), A minimum thermodynamic model for the bipolar seesaw, *Paleoceanography*, *18*(4), 1087, doi:10.1029/2003PA000920.

Vimeux, F., V. Masson, J. Jouzel, M. Stievenard, and J. R. Petit (1999), Glacial-interglacial changes in ocean surface conditions in the Southern Hemisphere, *Nature*, *398*, 410–413.

Vimeux, F., K. M. Cuffey, and J. Jouzel (2002), New insights into Southern Hemisphere temperature changes from Vostok ice cores using deuterium excess correction, *Earth Planet. Sci. Lett.*, *203*, 829–843.

Vimeux, F., V. Masson, G. Delaygue, J. Jouzel, J. R. Petit, and M. Stievenard (2001a), A 420,000 year deuterium excess record from East Antarctica: information on past changes in the origin of precipitation at Vostok, *J. Geophys. Res.*, *106*, 31,863–31,873.

Vimeux, F., V. Masson, J. Jouzel, J. R. Petit, E. J. Steig, M. Stievenard, R. Vaikmae, and J. W. C. White (2001b), Holocene hydrological cycle changes in Southern Hemisphere documented in East Antarctic deuterium excess records, *Clim. Dyn.*, *17*, 503–513.

Weaver, A. J., O. A. Saenko, P. U. Clark, and J. X. Mitrovica (2003), Meltwater pulse 1A from Antarctica as a trigger of the Bølling-Allerød warm interval, *Science*, *299*, 1709–1713.

Winter, A., and K. Martin (1990), Late Quaternary history of the Agulhas Current, *Paleoceanography*, *5*, 479–486.

Zielinski, U., R. Gersonde, R. Sieger, and D. Fütterer (1998), Quaternary surface water temperature estimations: Calibration of a diatom transfer function for the Southern Ocean, *Paleoceanography*, *13*, 365–383.

A. Abelmann, G. Cortese, and R. Gersonde, Alfred Wegener Institute for Polar and Marine Research (AWI), Columbusstrasse, P.O. Box 120161, D-27515 Bremerhaven, Germany. (gcortese@awi-bremerhaven.de)